AIMS Materials Science, 8(4): 550–559.
DOI: 10.3934/matersci.2021034
Received: 13 March 2021
Accepted: 02 June 2021
Published: 02 July 2021

http://www.aimspress.com/journal/Materials

Research article

Dependence the microstructure specifications of earth metal lanthanum La substituted $Bi_2Ba_2CaCu_{2-X}La_XO_{8+\delta}$ on cation vacancies

Raghad Subhi Abbas Al-Khafaji*, and Kareem Ali Jasim

University of Baghdad, College of Education for pure science Ibn-Al-Haitham, Department of Physics, Iraq

* **Correspondence:** Email: raghad@ihcoedu.uobaghdad.edu.iq.

Abstract: The paper delivers an analyzing and discussion of the experimental results for the effect of lanthanum substitution on the structural behavior for compounds ($Bi_2Ba_2CaCu_{2-X}La_XO_{8+\delta}$) with variation concentrations from 0 up to 0.2 with a fraction of 0.05. Specimens prepared by solid-state reaction. We investigate the structural properties, studying the lanthanum substitution instead of lead using the resulting properties of XRD. The sintering process was done below the melting point of any one of the component materials. The optimum sintering temperature was equal to 850 °C for 72 h to produce an active powder with higher densities and reduced the distance between the grains. (FWHM) results were calculated using X-ray information. The crystallite size D was estimated by Scherer and Williamson–Hall equations, where the results showed that the crystallite size (57.029–63.281 nm) and (56.395–65.948 nm) respectively, besides, the degree of crystallinity (41.64–63.79%) correlation with concentrations of lanthanum substitution. Through the outcome values, the results of the three methods are observed close to each other and this indicates that these methods are compatible with the compound and that the partial replacement occurs a noticeable change in the size of the crystallite as well as in the degree of crystallinity.

Keywords: structure behavior; sintering process; crystallite size; micro strain; crystallinity degree

1. Introduction

Morphology of crystal and particle size perform an energetic role in the applications, which has guide the scientists to concentrate on the production of materials. There are physical as well as chemical procedures have been used to synthesize the nanoparticles. Quantitative analysis characterized the phase compositions, parameters of crystal lattice, crystallite size and crystallinity degree of the materials. Particular methods employed in the quantitative analysis were Scherrer equation, Williamson–Hall method, Warren-Averbach analysis, Rietveld refinement and pseudo-Voigt function. However, Williamson–Hall (W–H) analysis of crystallite size and stress analysis is as yet under-utilized when contrasted to Scherer's equation. Amongst the several techniques practiced to measure crystallite sizes was X-ray diffractometer (XRD), stay a predominant manner for determining the size of crystallite. The chief characteristic take out from the XRD peak width analysis is the capillary strain. The crystallite size and lattice strain are measured the size of the coherent diffraction fields and the spreading of lattice constants from the lattice dislocations, in that order [1,2].

The first material to be discovered with a superconducting of high temperature without rare-earth component was the bismuth-based copper (BSCCO) [3]. Its crystal structure is formed by superconducting CuO_2 planes separated by layers of oxides of other chemical elements such as barium and calcium that crystallize according to the general chemical formula $Bi_2Sr_2Ca_{(n-1)}Cu_nO_{(2n+4+\delta)}$, where n is the number related to planes of CuO_2 in the unit crystal cell. Phases superconductive happen at different transition temperatures depending on the values of n (n = 1 (Bi-2201, Tc = 10 K), n = 2 (Bi-2212, Tc = 85 K), and n = 3 (Bi-2223), Tc = 110 K). Whereas the uppermost T_c value is for Bi-2223, the extremely investigated phase is Bi-2212 due to its advanced thermodynamic steadiness and comfortable manufacture path. The superconductivity characters of B-base systems, similar to other high temperature superconductor (HTS) containing the carrier of charge concentrations (CuO_2 planes), are strongly influenced by the valence measures. In particular, between the increased partial breakage of oxygen and the positive perturbation, the latter playing a dominant role in the process of formation of the stable supercomputer [4,5]. It should be noted that it is very difficult to obtain equal and accurate measurements in bulk compounds because, in addition to the starting composition, they may affect the preparation conditions such as sintering and heat treatment on the composition of the compound and the number of additional other preparation stages [6–8]. There are other homogeneous compounds with higher values of n obtained after substituting elements with other elements [6,7]. Besides, the crystallite sizes are greatly affected by the ionic radius when partially substituting calcium with barium, bismuth with lead and lanthanum La, with copper in the presence of Cu ions, so that the partial substitution has suitable values that allow maintaining the equilibrium of charges in the compound. Some elemental oxides were found that neutralized the stability of the compounds for a long time [8–12]. These results in promising enhancements: replacing Bi^{+3} with Pb^{+2} increasing the valence of copper and thus increases the number of aperture carriers of charge [8]. Accordingly, results in a significant advance of the critical current under the magnetic field when the optimum lead contents (x = 0.16), with no important difference in the transition temperatures T_c [13–15]. So that, majority of the presently manufactured and stable BSCCO compounds consist of the family of Pb-doped (Bi, Pb)-2212, and many investigate efforts are purposed at discovery other alternatives in the research to obtain further improvements such as higher transition temperature and increased stability of superconducting

compounds [8,13]. The crystal structure performing a prominent character in chemical stability of compounds and physical properties such as electrical conductivity. There are different ways to calculate the crystallite size within crystal structure. In this work, we study the effect of partial substitution of copper Cu with Lanthanum La through a concentration of 44 and 66 on the structural properties of $Bi_2Ba_2Ca\ Cu_{2-X}La_XO_{8+\delta}$ compounds with x = 0, 0.05, 0.10, 0.15 and x = 0.20 to calculate the crystallite size and micro strain values by employing Scherer and Williamson–Hall, furthermore, draw of size-micro strain.

2. Materials and methods

The synthesis of $Bi_2Ba_2CaCu_{2-X}La_XO_{8+\delta}$ compounds with x = 0, 0.05, 0.1, 0.15 and x = 0.2 were produced by solid-state-reaction procedure, and it is used suitable weights of 99% pure powder materials of BiO, BaO, CaO, CuO and LaO as the precursor materials with 99% purity. Where the mixing and grinding operations were carried out using a hand mixer, where the milling and combining process takes an hour. Using a whirlpool electric mixer contained steel balls for two hours, to produce fine powders along with the best consistency. The combination was dehydrated in an oven at 250 °C. After that the produced was pressed into a disc-shaped pellets (15 mm) with a diameter (2–3 mm) using a hydraulic press under pressure (6.5 tons/cm^2). Samples were placed in an electric furnace programmed for the purpose of sintering at 850 °C within 72 h, at a heating rate (10 °C/min) and below the pressure of normal atmospheric, to achieve samples with coherent and grantee an ideal diffusion procedure among the atoms, subsequently, the specimens were cooled to RT room temperature with the same rate. The structure of the ready samples was gain with an X-ray diffraction scale (XRD with an accuracy of 0.005) and within the range (10^o–80^o). By taking advantage of the Match program, XRD results in details were computed.

3. Results and discussion

XRD results can be drawn in the following Figure 1, the curve is between intensity and 2θ for $Bi_2Ba_2Ca\ Cu_{2-X}La_XO_{8+\delta}$ compounds with x from 0 up to 0.2 with increment 0.05, that the reflection H-peaks decrease and become it wide with increasing lanthanum concentration. Affording to the result of the XRD data, the structures of all specimens are orthorhombic and set up to comprise of close to pure phase $Bi_2Ba_2CaCu_2O_{8+\delta}$ (1212 phase) of polycrystalline. The patterns of the X-ray diffraction with Miller indices for x = 0, 0.05, 0.1, 0.15 and x = 0.2 are shown in Figure 1. Also there is an elimination of the peaks correspond to the impurity phases which leads to change in the crystallinity as well as to decrease the fraction peaks of major phase $Bi_2Ba_2CaCu_2O_{8+\delta}$ (H-phase 1212) and the following feature has been seen that the specimens possess more than one (phase major H-2212 and minor phase L-2201 and Small amount of impurity phases, that agreement with reference [11]. XRD gives us two kinds of information for the phases in samples in addition to their volume fractions and Lattice parameters a, b, and c of the corresponding phases as shown in Table 1.

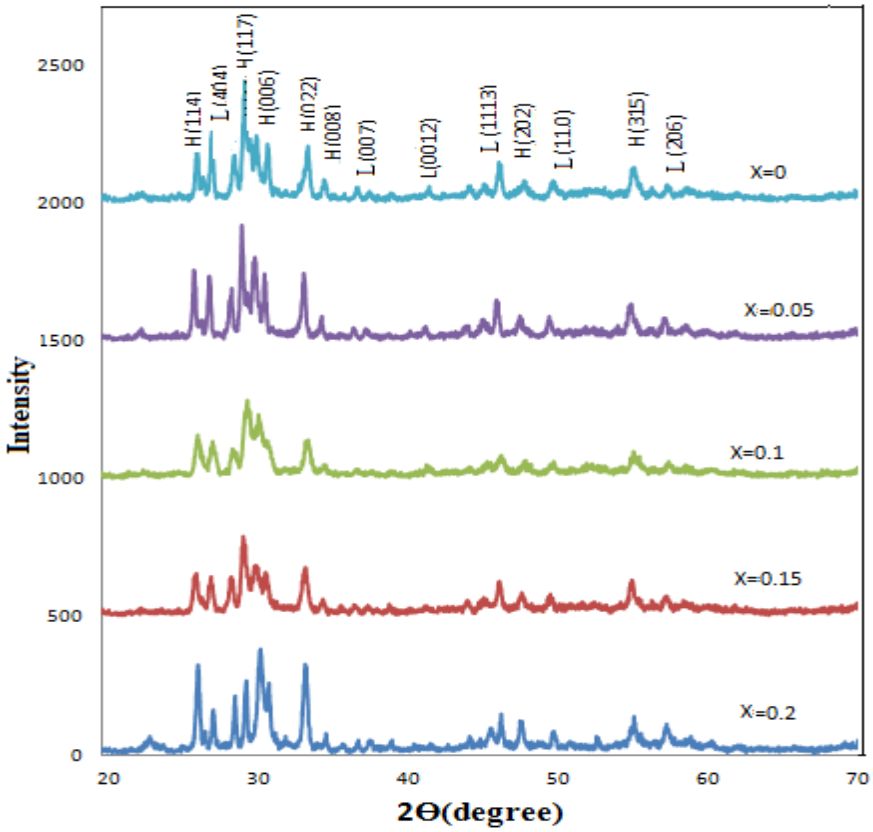

Figure 1. Intensity as function of 2θ for $Bi_2Ba_2CaCu_{2-X}La_XO_{8+\delta}$ compounds with x = 0, 0.05, 0.10, 0.15 and x = 0.20.

It is acknowledged that the parameters of a lattice are managed by the length of the plane (Cu–bond), and this length could be extended with the alter of electrons into defiant bonding orbitals, changing in parameters (a, b and c) effects on the unit cell volume, therefore, a variation caused in density, increasing of the density may be attributed to the reducing of the vacancies and porosity in the structure. The impurity values were computed as in our previous researches [7,9]. High and low phases as well as impurity results were draw corresponding to x concentrations of lanthanum La as illustrated in Figure 2. Furthermore, the relationship between the mass densities values as a function of La concentration which listed in Table 1, and plotted in Figure 3. It is noticed from the figure that the mass density has a value of 1.26 at x = 0 and falls to 1.17 when x = 0.05, But when the concentration of La is increased above this value, the density increases until it reaches 1.35 at x = 0.15 and then decreased to 1.19 at x = 0.20.

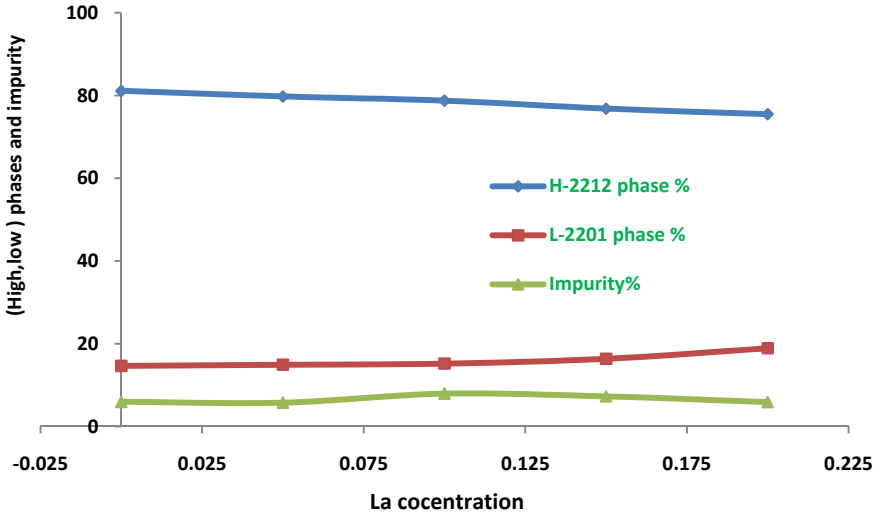

Figure 2. High and low phases as well as impurity verses concentrations x of lanthanum.

Table 1. Results of (high, low) phases, lattice parameters (a, b and c) and mass density ρ_M for $Bi_2Ba_2CaCu_{2-X}La_XO_{8+\delta}$ compounds with concentrations from 0 up to 0.2 with increment 0.05.

X	H%	L%	Impurity%	a (Å)	b (Å)	c (Å)	ρ_M (g/cm^3)
0	81.11	14.66	5.97	5.42	5.4509	23.23	1.26
0.05	79.74	14.94	5.76	5.71	5.4441	23.04	1.17
0.10	78.73	15.21	7.95	5.42	5.4956	23.01	1.29
0.15	76.81	16.37	7.28	5.40	5.4376	23.02	1.35
0.20	75.47	18.92	5.90	5.44	5.8173	22.89	1.19

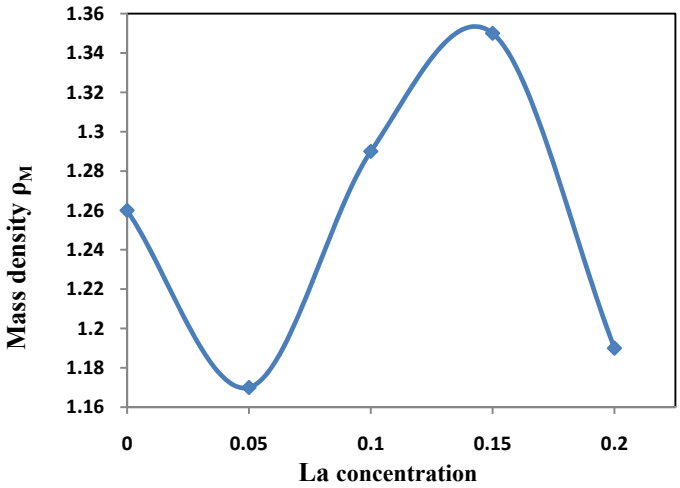

Figure 3. Mass density ρ_M as function of lanthanum La concentration for $Bi_2Ba_2CaCu_{2-X}La_XO_{8+\delta}$ compounds with x = 0, 0.05, 0.10, 0.15 and x = 0.20.

From Figure 1, the full-width-half-maximum (FWHM) values were calculated through the Origin Pro program by using X-ray output data. The crystallite size results were estimated by applying Scherer and Williamson–Hall equations, the peaks and their accompanying angles were determined, and after than calculating the $\cos\theta$ values of angles peaks and the values of $1/\beta_{hkl}$ for $Bi_2Ba_2CaCu_{2-X}La_XO_{8+\delta}$ compounds with x = 0, 0.05, 0.10, 0.15 and x = 0.20, from the Scherer equation [16,17]:

$$D = \frac{k\lambda}{\beta_{hkl}\cos\theta} \quad (1)$$

where Crystallite size (D), Scherer constant (k) = 0.9, X-ray wavelength (λ) = 1.540598 Å, Bragg angle (θ) and full-width-half-maximum (β_{hkl}).

The crystallite size values for all samples with different lanthanum La concentrations x = 0, 0.05, 0.10, 0.15 and x = 0.20 of the $Bi_2Ba_2CaCu_{2-X}La_XO_{8+\delta}$ compounds were listed in Table 2, using the Williamson–Hall equation [16–18]:

$$\beta_{hkl}\cos(\theta) = \frac{k\lambda}{D} + 4\,\varepsilon\sin(\theta) \quad (2)$$

where Micro strain (ε) values were calculated by plotting the relationship between $\beta_{hkl}\cos(\theta)$ for angles and $4\,\varepsilon\sin(\theta)$ for all lanthanum La concentrations.

The crystallinity can be computed through the following equation [18–20]:

$$\text{Degree of } crystallinity\ x_C\ \% = \frac{Area\ of\ Crystalline\ peaks\ \ A_C}{Area\ of\ all\ peaks\ (Crystalline\ A_C + Amorpous\ A_m)} \times 100 \quad (3)$$

where degree of crystallinity (x_C %), area of crystalline peaks (A_C) and area of amorphous peaks(A_m).

Table 2. Calculated values of (Scherer and Williamson Hall) crystallite size, micro strain and Degree of crystallinity for $Bi_2Ba_2CaCu_{2-X}La_XO_{8+\delta}$ compounds with x = 0, 0.05, 0.10, 0.15 and x = 0.20.

X	D-Scherrer (nm)	D-Williamson Hall (nm)	Micro strain	Degree of crystallinity %
0	57.029	56.395	0.0006	41.64
0.05	51.177	49.846	0.0004	47.26
0.10	58.343	59.126	0.0029	52.81
0.15	61.928	63.032	0.0004	59.46
0.20	63.281	65.948	0.0005	63.79

Figure 4 represents the relationship between the crystallite size calculated by the Scherer and Williamson–Hall methods from Eqs 1 and 2 as a function of the La concentration respectively, and the results reported in Table 1. Crystallite size values which obtained from Sharer equation will give smaller than that resulted from Williamson–Hall these referred to micro strain (non-uniform lattice distortions, faulting, dislocations, ant phase Domain, boundaries and grain surface relaxation) [21–24] which included in the second term of Eq 2. On the other hand, it is noticed from the Figure 4 that the crystallite size calculated by the two methods has a small value at x = 0.05 and increases as the concentration of La increases above this value. As shown in Table 2, results for the crystallite size

computed from the Scherer and Williamson–Hall micro strain and degree of crystallinity for $Bi_2Ba_2CaCu_{2-X}La_XO_{8+\delta}$ compounds with x = 0, 0.05, 0.10, 0.15 and x = 0.20 were summarized using Origin Pro 2019 software. In general, the average particle size changed as the concentration of La increased but there was also a change in the size of the crystallite when it was calculated by the three different methods. This could be due to the fine particles of $Bi_2Ba_2CaCu_{2-X}La_xO_{8+\delta}$ compounds being produced at a high value of phase 2212 and increasing the precursor-to-volume ratio to an increase in x ratio and this is due to the amount of defects and also vacancies in crystal such that are determined from the crystallite size using the Shearer equation.

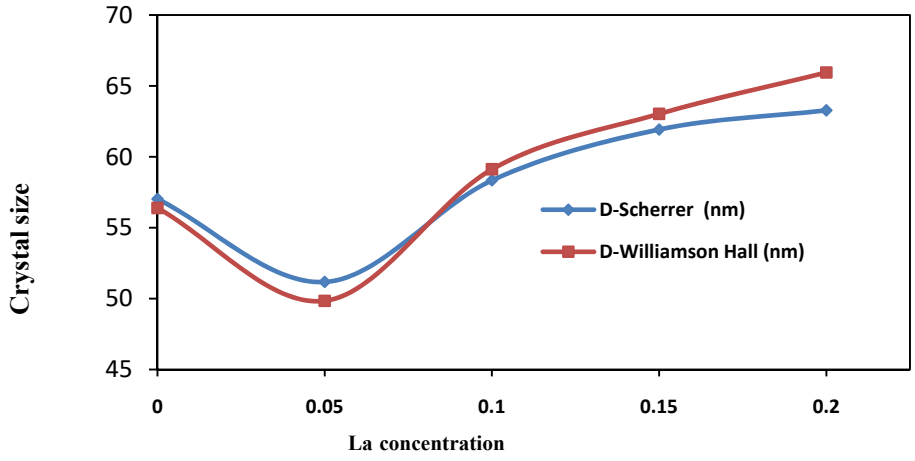

Figure 4. Crystallite size changed with lanthanum La concentrations x = 0, 0.05, 0.10, 0.15 and x= 0.20 of $Bi_2Ba_2CaCu_{2-X}La_XO_{8+\delta}$ compounds.

Figure 5 represents the relationship between degree of crystallinity values are computed from Eq 3 as a function of La concentration which recorded in Table 2. Where it is noticed from the Figure 5 that the degree of crystallinity increases as the concentration of La increases. The aim of using different methods to calculate the crystallite size is to know the method that gives the most accuracy in the calculations because each of these methods is compatible with one compound without the other. When observing the results of the crystallite size that were calculated by the three different methods, we conclude that all of these methods give close results and this indicates that these methods are consistent with the compound and that partial replacement takes place a noticeable change in the crystallite size as well as in the degree of crystallization and these results are in agreement with the results obtained in reference [14,25].

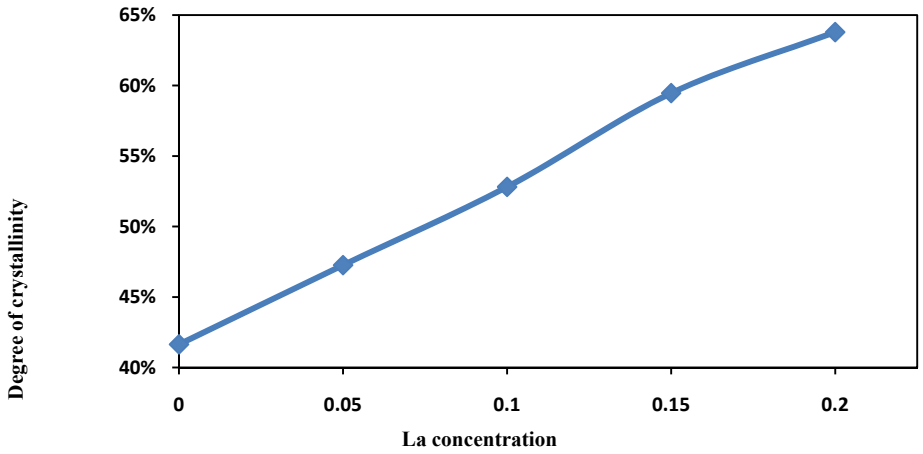

Figure 5. Degree of crystallinity as a function of lanthanum La concentrations for prepared compounds.

4. Conclusions

We have prosperously synthesized the compounds of $Bi_2Ba_2CaCu_{2-X}La_XO_{8+\delta}$ with x = 0, 0.05, 0.1, 0.15 and x = 0.2. Pallet Samples were prepared in the solid-state-manner were sintered at a firm temperature of 850 °C. The X-ray diffraction has identified the compounds, obtained results showed the crystal structure keeps on conformist on the orthotropic structures despite the change lanthanum La concentrations. The Full-width-half-maximum (FWHM) results were calculated with the benefit of the X-ray data. The crystallite size was estimated by using Scherrer and Williamson–Hall methods, it have a small value at x = 0.05 and increases as the concentration of La increases above this value, whereas the highest average of the size of crystallite 173.31 nm. The crystallinity and micro strain changing with change La concentrations. We conclude that all of these methods give close results and this indicates that these methods are consistent with the compound and that partial replacement takes place a noticeable change in the crystallite size as well as in the degree of crystallization

Conflict of interest

The authors will like to declare that this Article has no any financial or work related competing interest.

References

1. Kumar B, Hymavathi B (2018) X-ray peak profile analysis of solid-state sintered alumina doped zinc oxide ceramics by Williamson–Hall and size-strain plot methods. *J Asian Ceramic Soc* 5: 94–103.
2. Thang DV, Hung NM, Khang NC, et al. (2020) Structural and multiferroic properties of (Sm, Mn) co-doped $BiFeO_3$ materials. *AIMS Mater Sci* 7: 160–169.
3. Maeda H, Tanaka Y, Fukutomi M, et al. (1988) A new high-Tc oxide superconductor without a rare earth. *Jpn J Appl Phys* 27: L209.

4. Manfredotti C, Truccato M, Rinaudo G, et al. (2001) Annealing temperature dependence of the 2223 phase volume fraction in the Bi–Sr–Ca–Cu–O system. *Physica C* 353: 184–194.
5. Eisaki H, Kaneko N, Feng DL, et al. (2004) Effect of chemical inhomogeneity in bismuth-based copper oxide superconductors. *Phys Rev B* 69: 064512.
6. Togano K, Kumakura H, Maeda H, et al. (1988) Properties of Pb-doped Bi–Sr–Ca–Cu–O. superconductors. *Appl Phys Lett* 53: 1329.
7. Kareem KA, Tariq TJ, Al-Lamy HK, et al. (2011) Improvements of superconducting properties of $Hg_{0.6}Pb_{0.25}Sb_{0.15}Ba_2Ca_2Cu_3O_{8+\delta}$ ceramic. *J Supercond Nov Magn* 24: 1963–1966.
8. Cabassi R, Delmonte D, Abbas MM, et al. (2020) The role of chemical substitutions on Bi-2212 superconductors. *Crystals* 10: 462.
9. Jasim KA, Alwan TJ (2017) Effect of oxygen treatment on the structural and electrical properties of $Tl_{0.85}Cd_{0.15}Sr_2CuO_{5-\delta}$, $Tl_{0.85}Cd_{0.15}Sr_2Ca_2Cu_2O_{7-\delta}$ and $Tl_{0.85}Cd_{0.15}Sr_2Ca_2Cu_3O_{9-\delta}$ Superconductors. *J Supercond Novel Magn* 30: 3451–3457.
10. Coskun A, Ekicibil A, Özçelik B (2002) Superconductivity of $Bi_{1.6}Pb_{0.4}Sr_2Ca_3Cu_4O_{12}$. *Chinese Phys Lett* 19: 1863.
11. Li L, Lei L, Zhao G, et al. (2021) Microstructural characterization and superconducting properties of $GdBa_2Cu_3O_{7-x}$ films prepared by a fluorine-free sol-gel process. *Mater Charact* 172: 110899.
12. Ahsan MZ, Ahsan PM, Islam MA, et al. (2019) Structural and electrical properties of copper doped lanthanum manganite NPs. *Result Phys* 15: 102600.
13. Kumar J, Ahluwalia P K, Kishan H, et al. (2010) Significant improvement in superconductivity by substituting Pb at Bi-site in $Bi_{2-x}Pb_xSr_2CaCu_2O_8$ with x = 0.0 to 0.40. *J Supercond Novel Magn* 23: 493–499.
14. Eisaki H, Kaneko N, Feng DL, et al. (2004) Effect of chemical inhomogeneity in bismuth-based copper oxide superconductors. *Phys Rev B* 69: 064512.
15. Williamson GK, Hall WH (1953) X-ray line broadening from filed aluminium and wolfram. *Acta Metall* 53:22–31.
16. Vinila VS, Jacob R, Mony A, et al. (2014) X-ray diffraction analysis of nano crystalline ceramic $PbBaTiO_3$. *CSTA* 3: 57–65.
17. Bishnoi A, Kumar S, Joshi N (2017) Crystallite size and lattice strains from line broadening, In: Thomas S, Thomas R, Zachariah AK, et al., *Microscopy Methods in Nanomaterials Characterization*, Elsevier: 313–373.
18. Warren BE (1969) *X-Ray Diffraction*, Courier Corporation.
19. Crompton TR (2007) Toxicants in aqueous ecosystems: a guide for the analytical and environmental chemist, Springer.
20. Wang L, Su J, Guo Y, et al. (2021) 97.3% Pb-reduced $CsPb_{1-x}Ge_xBr_3$ perovskite with enhanced phase stability and photovoltaic performance through surface Cu doping. *J Phys Chem Lett* 12: 1098–1103.
21. Shafeek NA, Nawaf SF, Darweesh MH (2021) Fabrication of compound $Sn_{2-x}Ag_xSr_2Ca_2Cu_3O_{10+\&}$ superconductor by nano technique and study the nano and electrical properties. *Mater Today Proc* 42: 2797–2802.
22. Jasim KA, Thejeel MA, Al-Khafaji RS (2014) The effect of doping by Sr on the structural, mechanical and electrical characterization of $LaBa_{1-x}Sr_x\ Ca_2Cu_4O_{8.5+\delta}$. *IHJPAS* 27: 213–219.

23. Nikolay A (2020) Specialties of deformation and damage of the topocomposite on a ductile substrate during instrumental indentation. *AIMS Mater Sci* 7: 453–467.
24. Raghad SA (2013) Mechanical and electrical behavior of polymer matrix composite and their hybrids reinforced with (Carbon Black–Boron) particles. *ANJS* 16: 171–177.
25. Mustafa K, Kareem A (2020) Calculating of crystalline size, strain and degree of crystallinity of the compound ($HgBa_2Ca_2Cu_3O_{8+\sigma}$) by different method. *IOP Conf Ser Mater Sci Eng* 928: 072109.

AIMS Press